Cell, Volume *131*

Supplemental Data

Dynamic Scaffolding

in a G Protein-Coupled Signaling System

Prashant Mishra, Michael Socolich, Mark A. Wall, Jennifer Graves, ZiFen Wang, and Rama Ranganathan

Supplemental Experimental Procedures

Protein Expression and Purification

PDZ5 (residues 580-665 from *D.melanogaster* InaD) was cloned as a GST-fusion in pGEX-5X-3 (GE Healthcare) and expressed in *E.Coli* BL21-DE3 cells (Stratagene). Cells were grown at 37^{o}C in Terrific Broth to OD_{600} of ~1.2, induced with 100μm IPTG at 18ºC overnight, resuspended in PBS (10mM Na_2HPO_4, 1.8mM KH_2PO_4, 140mM NaCl, 2.7mM KCl, pH7.4) + 0.1% Tween-20, and lysed by sonication. The lysate was cleared by centriguation at 50,000g for 1 hour and incubated with glutathione sepharose (GE) at 4^{o}C for 1 hr. The resin was then washed with 20 bed volumes of PBS+0.1%Tween-20 followed by 20 bed volumes of PBS and eluted in PBS + 10mM reduced glutathione. To cleave the GST tag, Factor Xa protease (GE) was added at 1:50 (w/w) and the sample was dialyzed overnight into buffer A (50mM Tris, 100mM NaCl, pH7.5). Following rebinding to glutathione sepharose to remove undigested protein, the sample was subjected to size exclusion chromatography (Superdex 75, GE) in buffer A; fractions containing PDZ5 were pooled and concentrated in a Centricon YM-3 concentrator (Millipore) for crystallization trials. For the reduced state structure, buffer A was supplemented with 1mM dithiothreitol (DTT) during size-exclusion chromatography.

Selenomethionyl (SeMet) protein was produced for the reduced and C645S structures by growing cells in M9 minimal media at 37ºC to OD_{600} of 1.0, then incubating with amino acids (lysine, phenylalanine, threonine at 100mg/L; isoleucine, leucine, valine at 50mg/L, Se-methionine at 60mg/L) for 15 minutes, and finally inducing with 500μM IPTG overnight at 20ºC. Protein purification was carried out as above.

Structure Determination

Data were collected at 100ºK either at UT Southwestern Medical Center (oxidized structure, Table S1), beamline 1-5 at the Stanford Synchrotron Radiation Laboratory, SLAC (reduced structure, Table S2), beamline 19-BM at the Advanced Photon Source, Argonne National Laboratory (C645S structure, SeMet crystal, Table S3), or beamline 8.2.1 at the Advanced Light Source, Lawrence Berkeley Labs (C645S structure, native crystal, Table S3) and were indexed and scaled with DENZO/SCALEPACK (Otwinowksi, 1993). All phasing and model refinement was carried out with the Crystallography and NMR System (CNS) software (Brunger et al., 1998), and the statistics are summarized in Tables S1-S3.

For the 0mM DTT structure (Fig. 1C), automated Patterson search methods identified two Pt sites in an anomalous Patterson map; subsequently two more Pt sites and two Pd sites were identified on difference Fourier maps using the refined initial phases. After solvent flattening and phase extension to 2.1 Å, the experimental electron density map was easily traceable and showed 2 molecules in the asymmetric unit. For this and all subsequent PDZ5 structures (see below), no non-crystallographic symmetry restraints were used during phasing or refinement, and a randomly selected set of reflections (5%) was flagged for cross-validation. Manual model building was performed in O (Jones et al., 1991) and computational refinement steps involved high-temperature torsion angle molecular dynamics followed by positional and temperature factor minimization. After six rounds of refinement, the final model contained 85 residues for each

molecule and 153 water molecules. All figures and RMSD calculations were made in PyMol (DeLano, 2002). Atomic coordinates are deposited in the Protein Data Bank (accession code 2QKT).

The 10mM DTT structure (Fig. 2C) was determined using selenomethionine multi-wavelength anomalous dispersion methods. Here, automated Patterson search methods (CNS) identified all 6 selenium sites in an anomalous Patterson. After solvent flattening and phase extension to 2.2 Å, the experimental electron density map was clearly traceable and showed 3 molecules in the asymmetric unit. Model building and computational refinement were as described above. After seven refinement rounds, the final model contained 85, 84 and 90 residues for the three molecules plus 266 water molecules and 2 glycerol molecules. Atomic coordinates are deposited in the Protein Data Bank (accession code 2QKU).

The PDZ5^{Cys645Ser} structure (Fig. 3B) was determined using selenomethionine single wavelength anomalous dispersion methods. Automated Patterson search methods (CNS) identified all 4 selenium sites in an anomalous Patterson. Following solvent flattening and phase extension to 1.55 Å using data from a native crystal, the experimental electron density map was traceable and showed 2 molecules in the asymmetric unit. Model building and refinement was as above. After six rounds of refinement, the final model contained 92 residues for both molecules plus 181 water molecules. Atomic coordinates are deposited in the Protein Data Bank (accession code 2QKV).

Fly Stocks

The following fly stocks were used: wild-type (y^2w^1), InaD-null (y^2w^1; $inaD^1$), $inaD^2$, $inaD^{wt}$ (y^2w^1; $inaD^1$;$P[y^+,inaD^{wt}]$), $inaD^{C645S}$ (y^2w^1;$inaD^1$ $P[y^+,inaD^{C645S}]$), $ninaE^{I17}$, $inaC^{209}$, $arr2^3$, and $inaD^{C645S}$,$arr2^3$ (y^2w^1;$inaD^1$ $P[y^+,inaD^{C645S}]$;$arr2^3$). $inaD^{wt}$ and $inaD^{C645S}$ were constructed via standard P-element transformation using the YC4 vector (gift from Steve Britt; derived from the Y.E.S. vector (Patton et al., 1992)). The coding sequence of InaD, flanked by

the 5' and 3' UTRs of the Rh1 gene, was subcloned into YC4 and injected into y^2w^1; $inaD^1$ embryos. Transformants were homozygosed in an $inaD^1$ background using standard genetic crosses.

Stationary Fluctuation Analysis

Stationary fluctuation analysis was performed as previously described (Johnson and Pak, 1986; Juusola and Hardie, 2001; Wu and Pak, 1978); all calculations were performed in MatLab 7.0 (Mathworks Inc.). In brief, whole-cell recordings were collected from dark-adapted cells without series compensation. Data were recorded either in the dark or upon stimulation with 10 seconds of constant white light at intensities varying from $\log(I/I_0) = -8.5$ to $\log(I/I_0) = -6.0$ in steps of 0.5 log units. Data from the last 2 seconds of each exposure were used to extract average bump parameters using Campbell's theorem for rectangular shot processes, which relates the mean (μ) and variance (σ^2) of the observed current (after subtracting the background (dark) mean and variance) to three parameters – the bump amplitude (a), the bump duration (T), and the rate of bump generation (λ):

$$\mu = a\lambda T$$
$$\sigma^2 = a^2\lambda T$$

The amplitude, a, can then be calculated directly from the ratio of the variance to the mean. The bump duration, T, can be estimated from the spectral density function as described previously (Johnson and Pak, 1986; Juusola and Hardie, 2001; Wu and Pak, 1978); briefly, the experimental power spectrum is fit to a normalized single Lorentzian:

$$k\left(\frac{1}{1+(2\pi\tau f)^2}\right)^{n+1}$$

where f represents frequency; k, τ, n are parameters to be fit. T and λ can then be calculated as

$$T = \tau\frac{(n!)^2 2^{2n+1}}{(2n!)} \text{ and } \lambda = \frac{\mu}{aT}$$

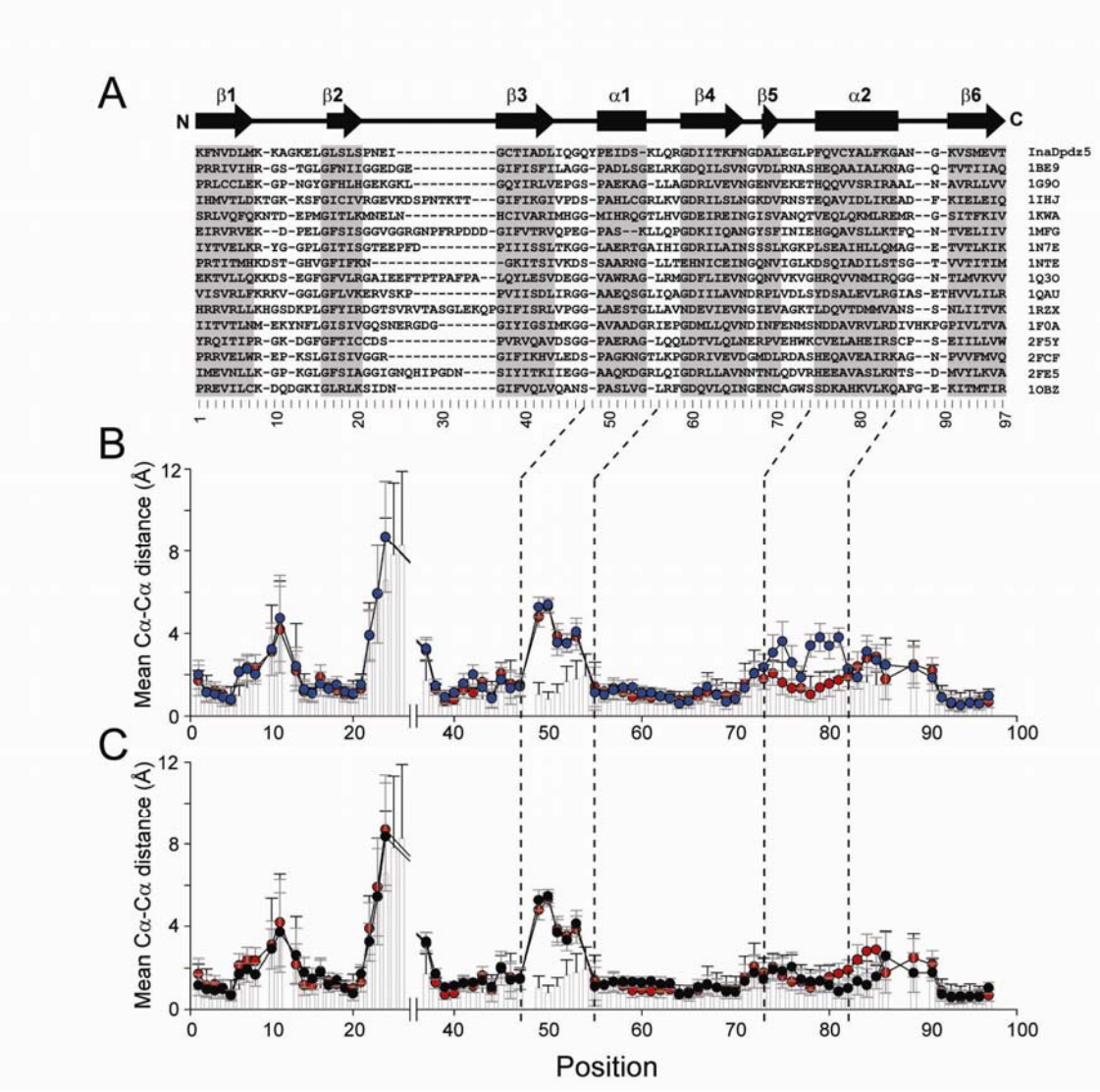

Figure S1. Comparison between INAD-PDZ5 and Known PDZ Domain Structures

(A) The RCSB protein data bank (http://www.rcsb.org/pdb) was searched for PDZ domain crystal structures with resolution < 2.5 angstroms and R_{free}<0.30. Sixteen manually aligned sequences (including PDZ5) are shown with their PDB accession codes listed on the right.

(B) Pairwise structural alignment of Cα atoms from the domains listed in (**A**) was performed in PyMol (DeLano Scientific, http://pymol.sourceforge.net/) using the 'fit' command. Cα-Cα distances were calculated from the fits and averaged. In grey are the distances calculated from all

pairwise alignments of domains not including PDZ5. In blue, the oxidized form of PDZ5 is compared with other PDZ domains. In red, the reduced form of PDZ5 is compared. Both forms show significant deviations in the region of the α1 helix; however, only the oxidized form shows deviations in the α2 helix. Bars indicate standard deviations.

(C) Similar calculations as in (**B**). In grey are the distances calculated from all pairwise alignments of domains not including PDZ5. In red, the reduced form of PDZ5 is compared with other PDZ domains; in black, $PDZ5^{C645S}$ is compared. Both the reduced form of PDZ5 and $PDZ5^{C645S}$ show significant deviations in the α1 helix, but not in the α2 helix. Bars indicate standard deviations.

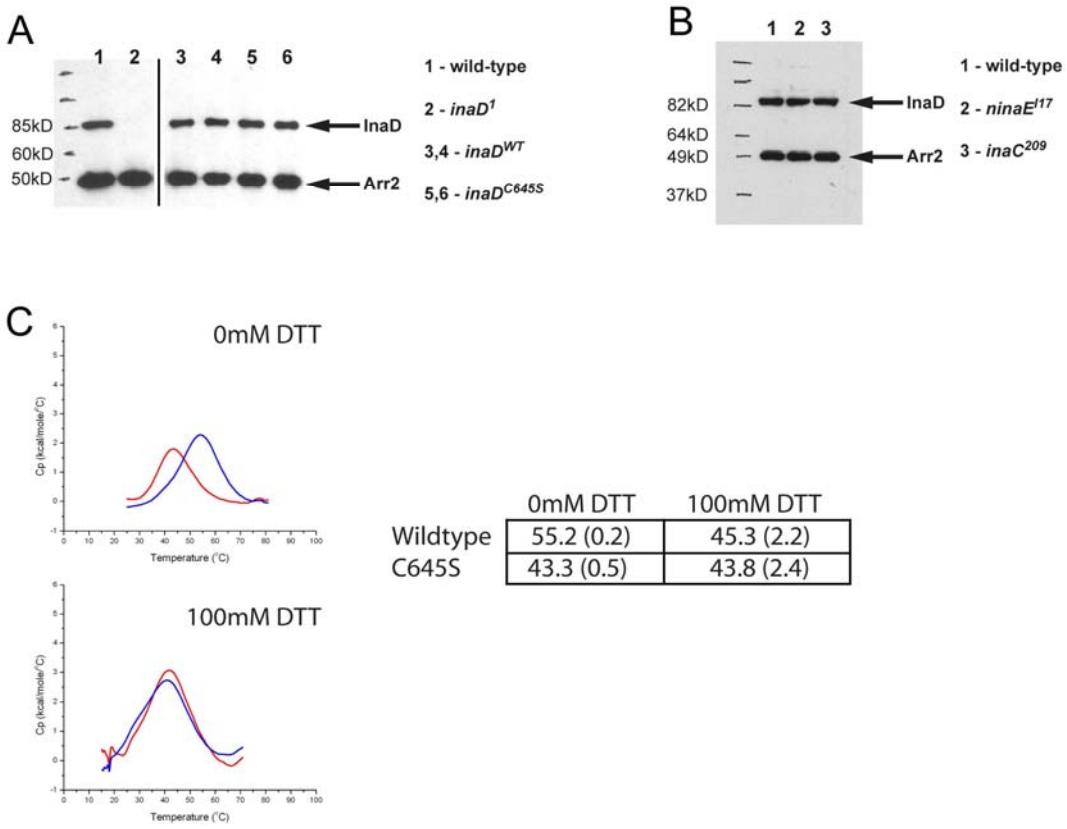

	0mM DTT	100mM DTT
Wildtype	55.2 (0.2)	45.3 (2.2)
C645S	43.3 (0.5)	43.8 (2.4)

Figure S2. InaD Protein Expression Levels in Flies and Characterization of the C645S Mutant Protein

(A) Western blots from fly head extracts. Homogenate from single fly heads was separated by 10% SDS-PAGE, transferred to PVDF membrane and probed with antibodies against the 1st PDZ domain of InaD and Arr2 (loading control). All transgenic flies (lanes 3-6) express levels of InaD comparable with wild-type.

(B) Western blots prepared as in (**A**). *ninaE*^{I17} flies, which are null for the major rhodopsin of the eye, and *inaC*^{209} flies, which are null for eye-PKC, express wild-type levels of InaD.

(C) Thermal stability of PDZ5. (Top) Wild-type (blue) or C645S (red) recombinant PDZ5 were assayed for thermal stability in the absence of DTT via differential scanning calorimetry (VP-DSC Capillary MicroCalorimeter (MicroCal, Inc.), scan rate 120°C/hr, filter period of 8sec). Normalized, baseline subtracted curves show a clear transition, indicating that wild-type PDZ5 has a higher melting temperature (T_m) and enthalpy of unfolding. (Bottom) Same as top panel, except 100mM DTT was included in buffer solutions, thereby reducing wild-type PDZ5. Similar T_ms are observed for wild-type and mutant (C645S) PDZ5. (Table) Summary of thermal stability experiments. Assays were performed in triplicate, mean T_m (°C) and standard deviation are reported. Oxidized PDZ5 is significantly more stable than reduced PDZ5 or mutant (C645S) PDZ5; however, no differences in stability are observed between C645S and reduced wild-type PDZ5.

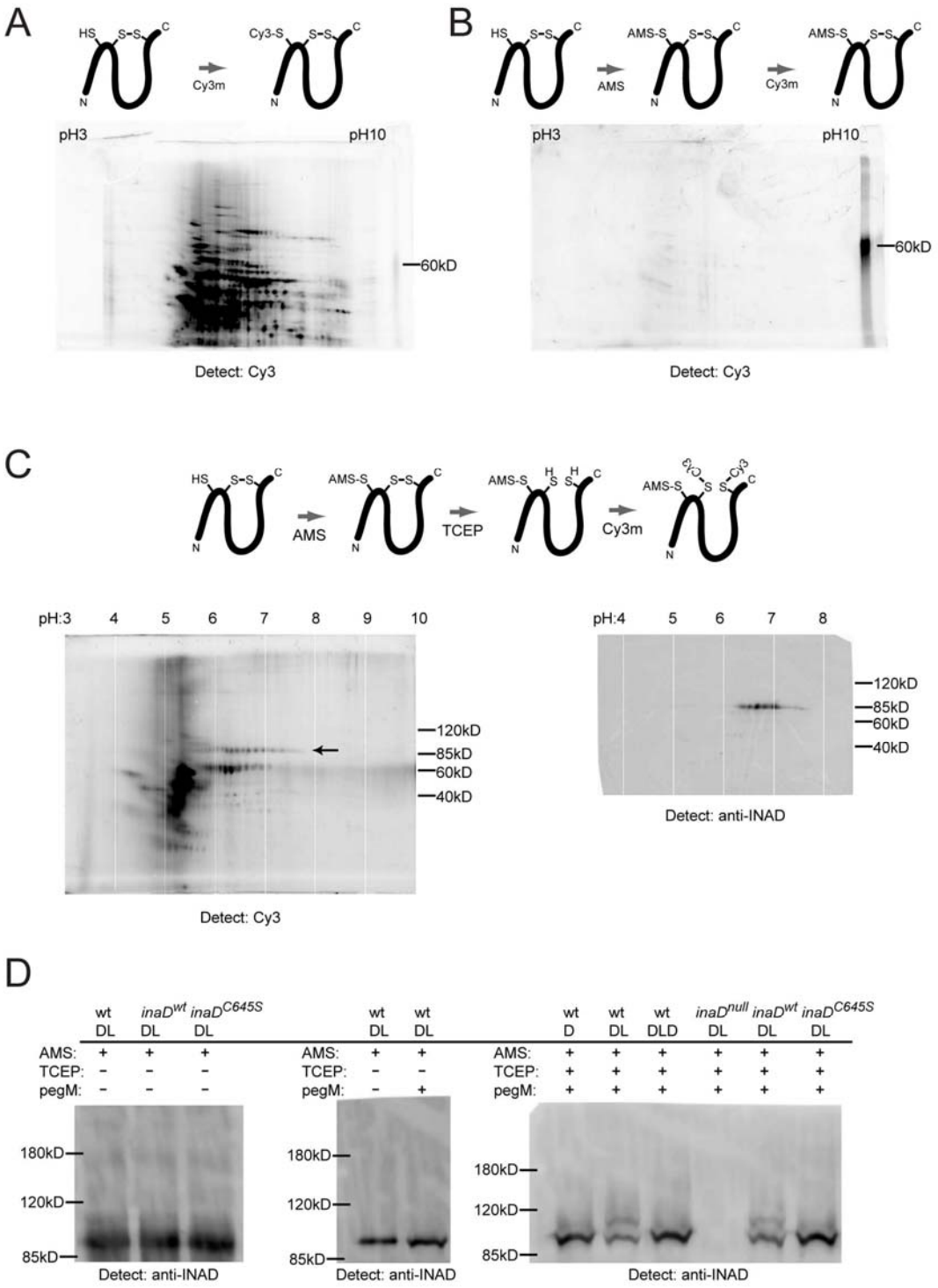

Figure S3. An Assay to Measure Disulfide Bond Formation In Vivo

(A) Total protein in *Drosophila* retinas was visualized by direct labeling with Cy3-maleimide (Cy3m). 2D gel electrophoresis followed by Cy3 detection shows the large number of protein species present in the *Drosophila* retina.

(B) Omission of TCEP in the disulfide assay (Fig. 4A) precludes any Cy3 labeling. Thus, any Cy3 labeling observed in Figs. 4B-I is specific to the disulfide reduction step.

(C) (left) Disulfide-bonded proteins in light-reared wild-type flies. A series of Cy3-labeled spots (arrow) appears in a position consistent with InaD (between pH6 and pH8 and a mobility of approximately 85kD). (right) Western-blot (probed against InaD) of a 2D gel from wild-type flies. InaD runs at 85kD, between pH6 and pH8.

(D) Similar assay as in (**C**), except a 5kD pegylated-maleimide (pegM, Sigma) is used in place of Cy3m. Western blots (probed against InaD) of non-reducing 1D SDS-PAGE gels are shown. (Left) TCEP and pegM are omitted. In this condition, we can examine InaD's participation in intermolecular disulfide bonds. The lack of higher molecular weight species (>85kD) indicate that InaD is not involved in an intermolecular disulfide bond, in either its wild-type or mutant (C645S) form. (Middle) Omission of TCEP precludes any labeling by pegM. Thus, pegM labeling of InaD (see below) is specific to the disulfide reduction step. (Right) With inclusion of TCEP, pegM will cause mobility shifts in disulfide-bonded proteins. Dark-reared (D) wild type flies show no shift, unless exposed to light (DL). When returned to dark conditions (DLD), wild-type flies again relax to a reduced state with no mobility shift. Light-exposed $inaD^{wt}$ flies show a mobility shift, while light-exposed $inaD^{C645S}$ flies do not. These results confirm the gels shown in Fig. 4.

Mishra et al., Figure S4

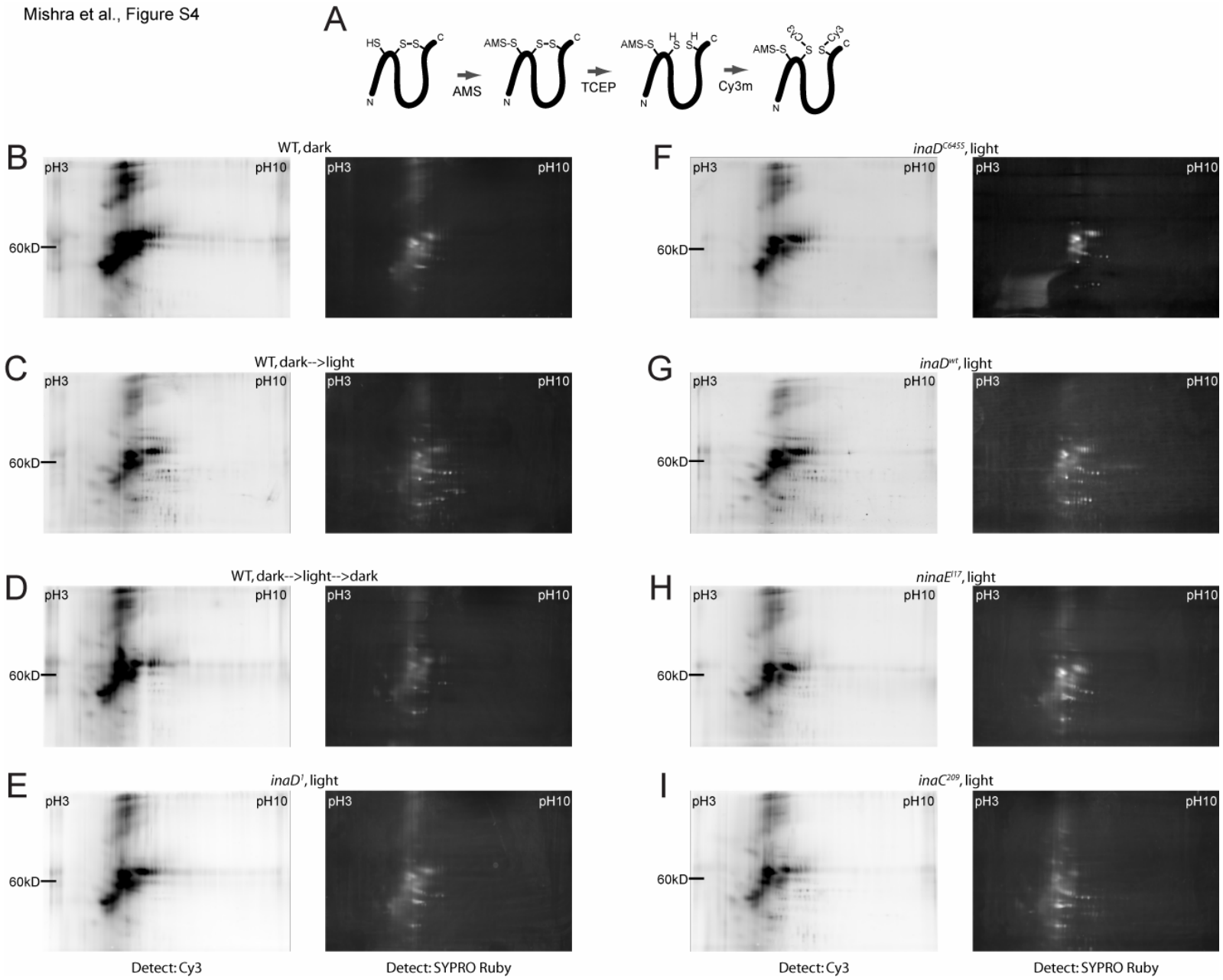

Figure S4. Visualization of Disulfide Bond Containing Proteins

(A) Schematic for specific labeling of disulfide bond containing proteins. Free cysteines are first blocked with the maleimide reagent (AMS); any disulfide bonds are then reduced with the reductant (TCEP) and labeled with the fluorescent reagent, Cy3-maleimide (Cy3m).

(B–I) Full gels for images in Figs. 4B-I. Shown on the left are 2D gels of disulfide containing proteins (visualized by Cy3 detection) from dark-reared wild-type flies (**B**), light-exposed wild-type flies (**C**), light-exposed wild-type flies returned to the dark for 30 minutes (**D**), light-exposed InaD-null flies (*inaD*^{1}) (**E**), light-exposed *inaD*^{C645S} flies (**F**), light-exposed *inaD*^{wt} flies (**G**), light-exposed *ninaE*^{I17} flies which are null for the major rhodopsin of the eye (**H**), and light-exposed *inaC*^{209} flies which are null for eye-PKC (**I**). The same gels were then fixed, stained for total protein using the SYPRO Ruby stain (Molecular Probes), and imaged (shown on right). Cy3 image intensities are normalized for total protein levels.

Figure S5. Cysteines in InaD and PLCβ

(A) Sequence alignments of the 1st and 5th PDZ domains of InaD from *D.melanogaster (Dm)* and the blowfly *Calliphora vicinia (Cv)*. The cysteine (red) implicated in a disulfide bond between the 1st PDZ domain and NorpA PLC-β (Kimple et al., 2001) is not conserved in *C.vicinia*, questioning its importance to visual signaling. The cysteines (red) involved in an intramolecular disulfide bond in the 5th PDZ domain are conserved in both species.

(B) Genomic sequencing of the C-terminus of *D.melanogaster* NorpA PLC-β. The genomic fragment was amplified from a y^2w^1 fly using the Polymerase Chain Reaction (PCR) and the following oligonucleotides (5'-TGTTGAGATAATTTCGAGCACGGTTTCGCG-3' and 5'-GGTATTAAGAATATAAGCTTATGCTTCCGGC-3'); the fragment was sequenced using the following oligonucleotide (5'-TCACCCCAAATCGCTAATGGC-3'). Sequencing was performed by the McDermott Center for Human Genetics (The University of Texas Southwestern Medical Center at Dallas). The arrow indicates Tyr1094 which was previously reported as Cys1094 (Bloomquist et al., 1988); this concurs with results from the Berkley Drosophila Genome Project (Celniker et al., 2002). Similar results indicate that position 1094 is a

phenylalanine in *C.vicinia* (A. Huber, personal communication). Thus, no intermolecular bond exists between the 1st PDZ domain of InaD (PDZ1) and NorpA PLC-β. Previous data indicating an interaction between PDZ1 and NorpA PLC-β concluded that binding was redox-dependent (Kimple et al., 2001). In light of the sequence data presented here, we conclude that there exists no evidence for an interaction between PDZ1 of InaD and NorpA PLC-β.

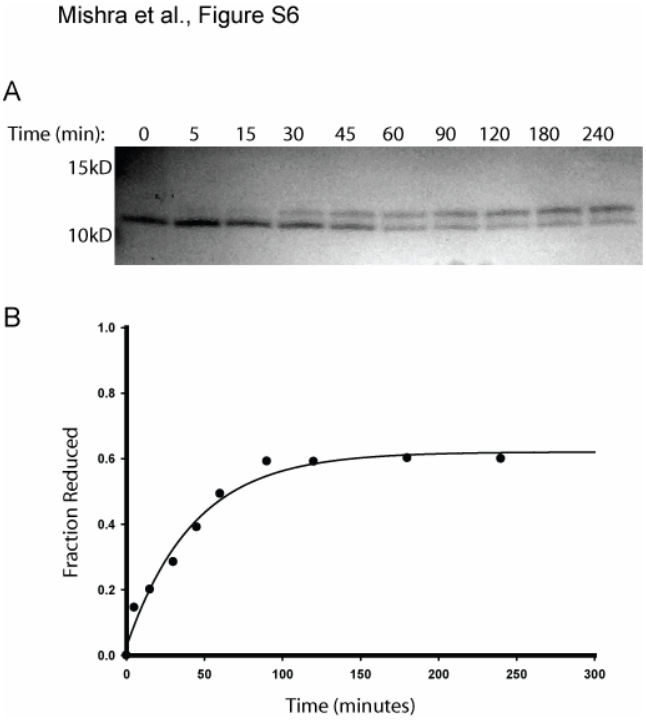

Figure S6. Establishment of Equilibrium Conditions for DTT Titration of PDZ5

(A) For titrations performed in Figure 2A, all reactions were incubated at 30°C for 4hr to reach equilibrium. Equilibrium was usually reached within 1-2 hours; for instance, PDZ5 incubated with 15mM DTT reaches equilibrium within 90 minutes.

(**B)** Quantitation of (**A**).

Tables S1–S3.

Crystallographic structure determination parameters and statistics for the no reductant (Table S1 and Fig. 1c, PDB 2QKT), 10mM DTT (Table S2 and Fig. 2c, PDB 2QKU), and C645S mutant (Table S3 and Fig. 3b, PDB 2QKV) PDZ5 domains.

Table S1, **PDZ5 structure, no DTT (PDB Accession Code 2QKT)**

Data Collection/Phasing:

Space Group:	$P4_12_12$			
Cell Dimensions	a=95.74 Å, b=95.74 Å, c=48.56 Å, α=β=γ=90.0°			
Dataset	Native	K_2PtCl_4	trans-$Pd(NH_3)_2Cl_2$	trans-$Pd(NH_3)_2Cl_2$
Source	Dip2020	RAXIS II	RAXIS II	Dip2020
Wavelength (Å)	1.54	1.54	1.54	1.54
Resolution range (Å)	20-2.05	20-2.4	20-2.05	20-2.3
Reflections (Unique)	209518 (14738)	154025 (16182)	158249 (16107)	122843 (18604)
Completeness				
All/Outer Shell	99.7/99.8	95.2/96.4	60.3/50.3	98.5/98.9
R_{sym} (%)[a]				
All/Outer Shell	4.4/15.3	7.6/23.7	4.9/37.5	5.8/22.0
I/σ				
All/Outer Shell	44.3/16.7	21.6/6.1	13.4/1.6	16.9/4.2
Heavy Atom Sites	--	4	2	2
R_{cullis}	--	0.80	0.92	0.97
Phasing Power (iso)	--	1.27	0.43	0.37
Phasing Power (ano)	--	1.23	0.71	0.30

Refinement

Dataset	Native
Resolution (Å)	2.05
Reflections working/test	13903/737
R (R_{free})[b]	0.224 (0.242)
No. of atoms	
Protein	1304
Waters	153
Mean B factor	27.5 $Å^2$
RMSD Bond Length	0.007 Å
RMSD Bond Angle	1.6°
Ramachandran outliers	0

[a] $R_{sym} = |I_h - \langle I_h \rangle| / I_h$, where $\langle I_h \rangle$ is the average intensity over symmetry equivalent reflections.
[b] $R = \Sigma|F_{obs} - F_{calc}|/\Sigma(F_{obs})$, where the summation is over the data used in refinement. R_{free} is the same statistic caclulated for the 5% of data excluded from refinement steps.

Table S2 - **PDZ5 Structure, 10mM DTT (PDB Accession Code 2QKU)**

Data Collection/Phasing:

Space Group:	$P4_322$			
Cell Dimensions	a=67.70 Å, b=67.70 Å, c=162.5 Å, α=β=γ=90.0°			
Source	SSRL BL 1-5			
	Peak	Edge	High remote	Low remote
Wavelength (Å)	.97965	.980035	.925256	1.06883
Resolution range (Å)	40-2.2	40-2.2	40-2.2	40-2.2
Reflections (Unique)	163831 (35925)	163970 (35987)	151097 (35471)	166696 (35921)
Completeness				
All/Outer Shell	97.9/96.2	98.0/96.3	96.9/93.3	97.9/96.0
R_{sym} (%)[a]				
All/Outer Shell	12.9/56.9	12.9/60.0	14.3/65.7	11.6/55.3
I/σ				
All/Outer Shell	9.0/1.9	9.0/1.9	7.4/1.5	10.4/2.1
No. of Se sites	6	6	6	6

Resolution	FOM[b]
4.60	0.74
3.45	0.71
3.22	0.65
3.05	0.60
2.88	0.53
2.76	0.47
2.64	0.42
2.53	0.38
2.41	0.34
2.30	0.30

Refinement

Dataset	Low remote
Resolution limit (Å)	2.2
Reflections working/test	33753/1700
R (R_{free})[c]	0.206 (0.231)
No. of atoms	
Protein	1989
Waters	266
Glycerol	12 (2 molecules)
Mean B factor	24.0 Å^2
RMSD Bond Length	0.006 Å
RMSD Bond Angle	1.3°
Ramachandran outliers	0

[a] $R_{sym} = |I_h - \langle I_h \rangle| / I_h$, where $\langle I_h \rangle$ is the average intensity over symmetry equivalent reflections.
[b] Figure of Merit
[c] $R = \Sigma|F_{obs} - F_{calc}|/\Sigma(F_{obs})$, where the summation is over the data used in refinement. R_{free} is the same statistic caclulated for the 5% of data excluded from refinement steps.

Table S3 - **PDZ5 C645S Structure, no DTT (PDB Accession Code 2QKV)**

Data Collection/Phasing:

	Native	Se-Met
Space Group	$P4_32$	$P4_32$
Cell Dimensions	a=b=c=112.04 Å, $\alpha=\beta=\gamma=90.0^o$	a=b=c=112.05 Å, $\alpha=\beta=\gamma=90.0^o$
Source	ALS 8.2.1	APS 19-BM
Wavelength (Å)	1.0	0.97940 (peak)
Resolution range (Å)	40-1.55	40-2.01
Reflections (Unique)	559574 (36464)	273593 (16616)
Completeness		
All/Outer Shell	99.9/99.9	99.8/99.1
R_{sym} (%)[a]		
All/Outer Shell	5.2/50.4	5.1/10.5
I/σ		
All/Outer Shell	51.1/4.4	72.3/23.6
No. of Se sites	--	4

Resolution (Å)	Phasing Power	FOM[b]
4.00	6.23	0.47
3.18	4.81	0.49
2.77	4.55	0.50
2.52	4.32	0.51
2.34	3.78	0.49
2.20	3.30	0.46
2.09	2.93	0.43
2.00	4.42	0.34

Refinement

Dataset	Native
Resolution limit (Å)	1.55
Reflections working/test	30072/3324
R (R_{free})[c]	0.248 (0.267)
No. of atoms	
Protein	1406
Waters	181
Mean B factor	24.66 $Å^2$
RMSD Bond Length	0.007 Å
RMSD Bond Angle	1.7^o
Ramachandran outliers (Generously allowed / Disallowed regions)	2/0

[a] $R_{sym} = |I_h - \langle I_h \rangle|/I_h$, where $\langle I_h \rangle$ is the average intensity over symmetry equivalent reflections.
[b] Figure of Merit
[c] $R = \Sigma|F_{obs} - F_{calc}|/\Sigma(F_{obs})$, where the summation is over the data used in refinement. R_{free} is the same statistic caclulated for the 5% of data excluded from refinement steps.

Table S4. Structural Comparison between PDZ5 Structures and Other PDZ Domains

		Normal	PDZ5 oxidized	PDZ5 reduced	PDZ5 C645S
β2	K590	3.84 (1.54)	3.23 (1.26)	3.11 (1.14)	2.91 (0.96)
	L595	0.99 (0.39)	1.09 (0.44)	1.15 (0.42)	1.48 (0.52)
	L597	0.91 (0.39)	1.31 (0.37)	1.39 (0.39)	1.18 (0.35)
	S598	0.98 (0.43)	1.52 (0.40)	1.23 (0.33)	1.42 (0.30)
	L599	1.00 (0.41)	1.16 (0.35)	1.03 (0.34)	1.03 (0.31)
α2	F642	1.78 (0.82)	**3.60 (0.96)**	1.62 (0.57)	1.86 (0.63)
	C645	1.35 (0.57)	**3.41 (0.55)**	1.04 (0.35)	1.34 (0.42)
	Y646	1.47 (0.61)	**3.80 (0.67)**	1.37 (0.55)	1.38 (0.48)
	F649	1.28 (0.58)	**2.27 (0.48)**	1.85 (0.49)	1.02 (0.50)

In order to compare InaD PDZ5 with other known PDZ domains, we constructed structural alignments between PDZ5 and available PDZ structures (see Figure S1). Here, we report Cα-Cα distances (mean and standard deviation) for positions involved in ligand binding (numbering according to InaD). In the "Normal" column, PDZ structures (not including InaD PDZ5) are compared against one another to determine the variability in position for each residue. In the "PDZ5" columns, the indicated structure of PDZ5 is compared against other PDZ structures. In red are PDZ5 positions which differ from the "Normal" statistics by greater than one standard deviation. The oxidized form of PDZ5 differs from other PDZ domains in the α2 helix, while the reduced and mutant (C645S) forms show no significant differences. For a complete analysis of all positions, see Figure S1.

Supplemental References

Bloomquist, B. T., Shortridge, R. D., Schneuwly, S., Perdew, M., Montell, C., Steller, H., Rubin, G., and Pak, W. L. (1988). Isolation of a putative phospholipase C gene of Drosophila, norpA, and its role in phototransduction. Cell *54*, 723-733.

Brunger, A. T., Adams, P. D., Clore, G. M., DeLano, W. L., Gros, P., Grosse-Kunstleve, R. W., Jiang, J. S., Kuszewski, J., Nilges, M., Pannu, N. S., *et al.* (1998). Crystallography & NMR system: A new software suite for macromolecular structure determination. Acta Crystallogr D Biol Crystallogr *54*, 905-921.

Celniker, S. E., Wheeler, D. A., Kronmiller, B., Carlson, J. W., Halpern, A., Patel, S., Adams, M., Champe, M., Dugan, S. P., Frise, E., *et al.* (2002). Finishing a whole-genome shotgun: release 3 of the Drosophila melanogaster euchromatic genome sequence. Genome Biol *3*, RESEARCH0079.

DeLano, W. L. (2002). The PyMOL Molecular Graphics System (San Carlos, CA, USA: DeLano Scientific).

Johnson, E. C., and Pak, W. L. (1986). Electrophysiological study of Drosophila rhodopsin mutants. J Gen Physiol *88*, 651-673.

Jones, T. A., Zou, J. Y., Cowan, S. W., and Kjeldgaard (1991). Improved methods for building protein models in electron density maps and the location of errors in these models. Acta Crystallogr A *47 (Pt 2)*, 110-119.

Juusola, M., and Hardie, R. C. (2001). Light adaptation in Drosophila photoreceptors: I. Response dynamics and signaling efficiency at 25 degrees C. J Gen Physiol *117*, 3-25.

Kimple, M. E., Siderovski, D. P., and Sondek, J. (2001). Functional relevance of the disulfide-linked complex of the N-terminal PDZ domain of InaD with NorpA. Embo J *20*, 4414-4422.

Otwinowksi, Z. (1993). In Data collection and processing, L. Sawyer, Isaacs, N. & Bailey, S., ed. (Warrington, UK), pp. 56-62.

Patton, J. S., Gomes, X. V., and Geyer, P. K. (1992). Position-independent germline transformation in Drosophila using a cuticle pigmentation gene as a selectable marker. Nucleic Acids Res *20*, 5859-5860.

Wu, C. F., and Pak, W. L. (1978). Light-induced voltage noise in the photoreceptor of Drosophila melanogaster. J Gen Physiol *71*, 249-268.